

# The lithium isotope ratio in the metal-poor halo star G271-162 from VLT/UVES observations \*

P.E. Nissen<sup>1</sup>, M. Asplund<sup>2</sup>, V. Hill<sup>3</sup>, and S. D'Odorico<sup>3</sup>

<sup>1</sup> Institute of Physics and Astronomy, University of Aarhus, DK-8000 Aarhus C, Denmark (pen@ifa.au.dk)

<sup>2</sup> Uppsala Astronomical Observatory, Box 515, SE-751 20, Sweden (martin@astro.uu.se)

<sup>3</sup> European Southern Observatory, Karl-Schwarzschild Str. 2, D-85748 Garching b. München, Germany (vhill@eso.org, sdodoric@eso.org)

Received March 15 2000/ Accepted April 12 2000

**Abstract.** A high resolution ( $\lambda/\Delta\lambda \simeq 110\,000$ ), very high  $S/N$  ( $\gtrsim 600$ ) spectrum of the metal-poor turnoff star G 271-162 has been obtained in connection with the commissioning of UVES at VLT/Kueyen. Using both 1D hydrostatic and 3D hydrodynamical model atmospheres, the lithium isotope ratio has been estimated from the Li I 670.8 nm line by means of spectral synthesis. The necessary stellar line broadening (1D: macroturbulence + rotation, 3D: rotation) has been determined from unblended K I, Ca I and Fe I lines. The 3D line profiles agree very well with the observed profiles, including the characteristic line asymmetries. Both the 1D and 3D analyses reveal a possible detection of  ${}^6\text{Li}$  in G 271-162,  ${}^6\text{Li}/{}^7\text{Li} = 0.02 \pm 0.01$  ( $1\sigma$ ). It is discussed if the smaller amount of  ${}^6\text{Li}$  in G 271-162 than in the similar halo star HD 84937 could be due to differences in stellar mass and/or metallicity or whether it may reflect an intrinsic scatter of  ${}^6\text{Li}/{}^7\text{Li}$  in the ISM at a given metallicity.

**Key words:** Stars: abundances – Stars: atmospheres – Stars: fundamental parameters – Stars: individual: G271-162 – cosmic rays

## 1. Introduction

Due to the special status of  ${}^6\text{Li}$  for astrophysics and cosmology, much work has been devoted to the search for this isotope in metal-poor stars ever since the first detection in HD 84937 by Smith et al. (1993). The reason for this interest is threefold: *i*) The presence of  ${}^6\text{Li}$  in the envelope of halo stars severely limits the possible depletion of  ${}^7\text{Li}$ , and thus allows a more accurate determination of the primordial  ${}^7\text{Li}$  abundance (Ryan et al. 1999; Asplund & Carlsson 2000); *ii*)  ${}^6\text{Li}$  abundances provide an additional test of theories for the production of the light elements (Li, Be and B) by cosmic ray processes; *iii*) Since  ${}^6\text{Li}$  is an even more fragile nuclei than  ${}^7\text{Li}$  it is a sensitive probe of possible mixing events during the stellar life.

To date  ${}^6\text{Li}$  is claimed to have been detected in two metal-poor halo stars, HD 84937 and BD +26 3578, and two metal-

*Send offprint requests to:* P.E. Nissen

\* Based on public data released from the UVES commissioning at the VLT/Kueyen telescope, ESO, Paranal, Chile

poor disk stars, HD 68284 and HD 130551 (Smith et al. 1998; Hobbs & Thorburn 1997; Cayrel et al. 1999; Nissen et al. 1999). Clearly, an observational test of models for the formation and evolution of  ${}^6\text{Li}$  and for the depletion of  ${}^6\text{Li}$  in stellar envelopes requires a much larger set of  ${}^6\text{Li}$  data spanning a large metallicity range. With the advent of high-resolution spectrographs on 8m-class telescopes this is now becoming feasible.

The determinations of  ${}^6\text{Li}$  abundances are based on the increased width and asymmetry of the Li I 670.8 nm doublet introduced by the isotope shift ( $0.16\text{ \AA} = 7.1\text{ km s}^{-1}$ ) of  ${}^6\text{Li}$ . Since the line is not resolved, the derived  ${}^6\text{Li}$  abundance depends on the adopted stellar line broadening as estimated from other spectral lines. Until now all such analyses have relied on 1D hydrostatic model atmospheres which cannot predict the inherent line asymmetries introduced by the convective motions in the atmosphere and thus is a potential source of uncertainty. An attractive alternative is provided by the new generation of 3D hydrodynamical model atmospheres (e.g. Stein & Nordlund 1998; Asplund et al. 1999, 2000) which self-consistently compute the time-dependent convective velocity fields and thus are able to predict the convective line asymmetries.

In the present *Letter* we analyze a high resolution, very high  $S/N$  spectrum of the metal-poor halo star G271-162 obtained during the commissioning of UVES on VLT/Kueyen using both 1D and 3D model atmospheres. Thereby we also investigate the ability of UVES to provide high quality spectra as needed in many astrophysical studies.

## 2. Observations and reductions of UVES spectra

The metal-poor star G 271-162 (BD –10 388) was chosen as one of the targets for the first commissioning of UVES, the UV-Visual Echelle Spectrograph (D'Odorico & Kaper, 2000) on the ESO VLT UT2 (Kueyen) telescope. The aim was to test if UVES can supply high quality spectra suitable for a determination of the lithium isotope ratio in stars – one of the most demanding problems in observational stellar astrophysics. Being situated at the turnoff point for halo stars in the HR diagram, G 271-162 is very similar to HD 84937; hence, one would expect the Li isotope ratio to be about the same, i.e.

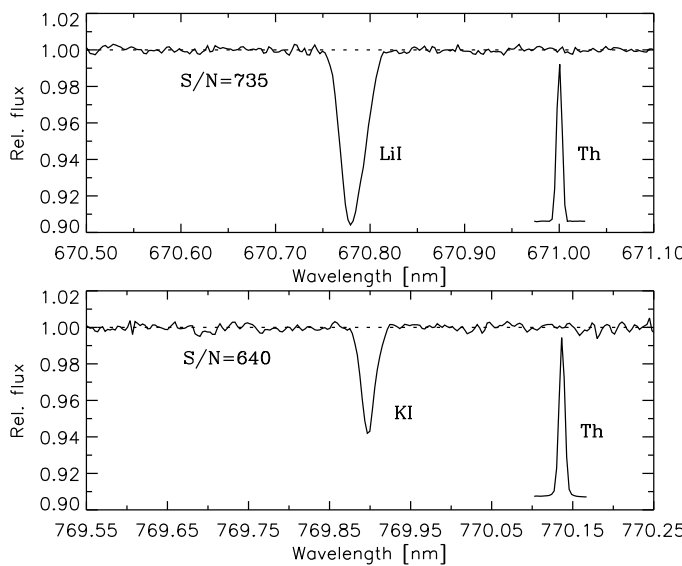


**Fig. 1.** UVES spectrum of G 271-162 in the regions of the Li I 670.8 and K I 769.9 nm lines with nearby thorium emission lines inserted

${}^6\text{Li}/{}^7\text{Li} \simeq 0.06$ . Furthermore, G 271-162 represents a group of about 50 halo turnoff stars with  $10 \lesssim V \lesssim 11.5$  that are too faint to be searched for  ${}^6\text{Li}$  using high resolution spectrographs at 4m class telescopes. With UVES it should be possible to reach these stars and hence to increase the sample of stars with  ${}^6\text{Li}$  determinations by an order of magnitude.

Four spectra of G 271-162 were obtained on October 11 - 13, 1999, with exposure times ranging from 30 to 60 min. The width of the entrance slit was set at 0.3 arcsec to get a resolution close to 120 000. An image slicer is foreseen for this high resolution mode of UVES, but was not available during the first commissioning run. Instead, the star was continuously moved along the slit within  $\pm 5$  arcsec corresponding to approximately 50 pixels on the CCDs. This widening of the echelle orders is essential in obtaining very high S/N. The lack of the image slicer made the efficiency of UVES critically dependent on the seeing, but it is noted that on one night with excellent seeing on Paranal (0.35 arcsec) the efficiency of UVES was as high as could be expected in the image slicer mode for average seeing conditions.

The red arm of UVES was applied with the two CCDs (EEV 4096  $\times$  2048 and MIT-LL 4096  $\times$  2048) covering the spectral regions 610 - 705 and 715 - 810 nm in 14 and 10 echelle orders, respectively. Cross disperser #3 was chosen to provide ample space ( $\simeq 150$  pixels) between the orders for accurate measurement of the background.

The spectra have been reduced using standard IRAF tasks for order definition, background subtraction, FF division, extraction of orders, wavelength calibration and continuum normalization. The spectrum of a bright B-type star, HR 8858, was observed and used to remove telluric lines present in some spectral regions. After correction for radial velocity shifts the

four spectra were combined to one. Fig. 1 shows the very high S/N and resolution obtained.

The wavelength calibration is based on 30-40 thorium lines per echelle order, and the rms of a 2-dimensional 4th order polynomial fit between pixel and wavelength space is 1.1 mÅ. In addition, the Th lines can be used to check the resolution; the instrument profile is well approximated with a Gaussian and no asymmetry is seen. The resolution as measured from the FWHM of the Th lines varies, however, along a given spectral order from about 100 000 to 120 000. Thanks to the large number of Th lines available, the variation could be mapped and the actual instrumental resolution for a given stellar line determined and applied in connection with the spectrum synthesis. It is noted that this problem of resolution variations has been fixed during the second commissioning run of UVES.

### 3. Analysis

The analysis of the Li I feature (equivalent width 29.0 mÅ) has been carried out using both 1D hydrostatic (Asplund et al. 1997) and 3D hydrodynamical LTE model atmospheres (Asplund et al. 1999). According to Strömgren photometry the stellar parameters of G 271-162 are  $T_{\text{eff}} = 6295 \pm 70$  K and  $[\text{Fe}/\text{H}] = -2.15 \pm 0.2$  while the uncertain Hipparcos parallax suggests  $\log g = 3.7_{-0.7}^{+0.4}$ . G 271-162 closely resembles HD 84937 for which the IR flux method (IRFM), the Hipparcos parallax and stellar spectroscopy imply  $T_{\text{eff}} = 6330 \pm 80$  K,  $\log g = 4.0 \pm 0.1$  and  $[\text{Fe}/\text{H}] = -2.25 \pm 0.2$ , which we therefore also adopt for G 271-162. It should be emphasized though that the exact choice of parameters does not influence significantly the lithium *isotope ratio* determinations although it does of course affect the *absolute* abundances.

When applying 1D model atmospheres to spectral synthesis additional line broadening besides the instrumental broadening is required. This broadening, which is mainly due to macro-turbulence, was approximated by a Gaussian function and determined from a  $\chi^2$  fit of five unblended lines (Ca I 612.2, Ca I 616.2, Fe I 623.0, Ca I 643.9, and K I 769.9 nm), all of similar strength as the Li I 670.8 nm line. In the case of the K I 769.9 nm resonance line the hyperfine structure and isotopic shift between  ${}^{39}\text{K}$  and  ${}^{41}\text{K}$  were taken into account although the effect turned out to be rather negligible. A more sophisticated broadening like a radial-tangential profile did not improve the agreement with the observed profiles. In contrast, in hydrodynamical model atmospheres the self-consistent convective motions account for all of the line broadening except for the unknown rotational velocity  $v_{\text{rot}} \sin i$  of the star. This parameter was determined by fitting a disk-integration of the angle-dependent theoretical 3D line profiles to the observed profiles of the K I, Ca I and Fe I lines.

The comparison between theoretical and observed profiles was quantified using a  $\chi^2$  analysis in an analogous way to previous investigations (Nissen et al. 1999). The  $\chi^2$  was computed through  $\chi^2 = \sum (O_i - S_i)^2 / \sigma^2$ , where  $O_i$  is the observed spectral point,  $S_i$  the synthesis and  $\sigma = (S/N)^{-1}$  as estimated in two adjacent continuum windows to the lines. When estimat-

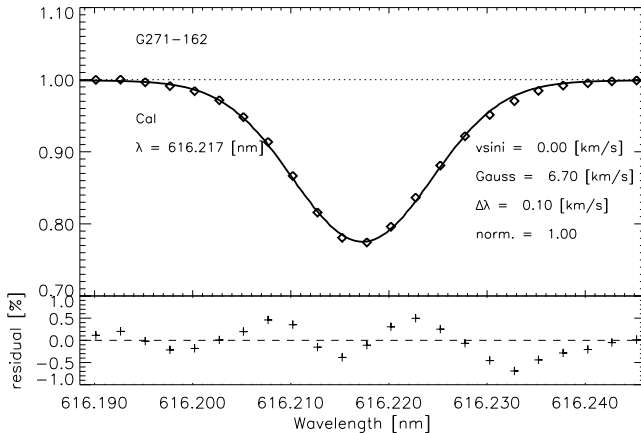


**Fig. 2.** The predicted (solid line) and observed (diamonds) Ca I 616.2 nm line together with the residual fluxes based on the 1D analysis. The Gaussian broadening with which the theoretical spectrum has been convolved include the combined effects of macroturbulence, rotation and instrumental resolution. Note the remaining systematic signal in the residuals

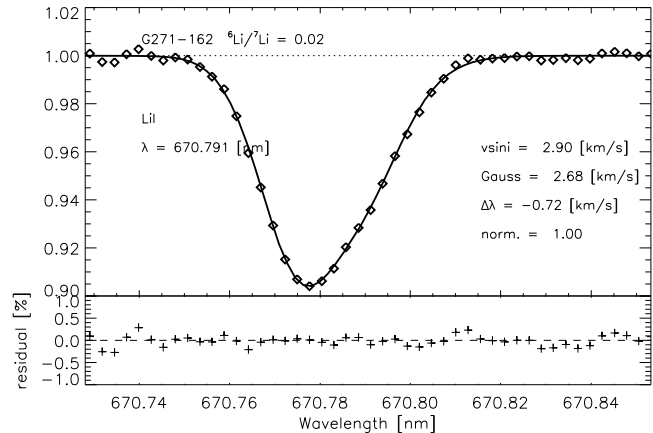


**Fig. 4.** The predicted (solid line) and observed (diamonds) Li I 670.8 nm lines together with the residual fluxes for the best fit with  ${}^6\text{Li}/{}^7\text{Li} = 0.02$  in the 3D analysis. The Gaussian broadening with which the theoretical spectrum has been convolved include only the instrumental resolution while the rotational broadening has been applied following a full disk-integration of the 3D profiles

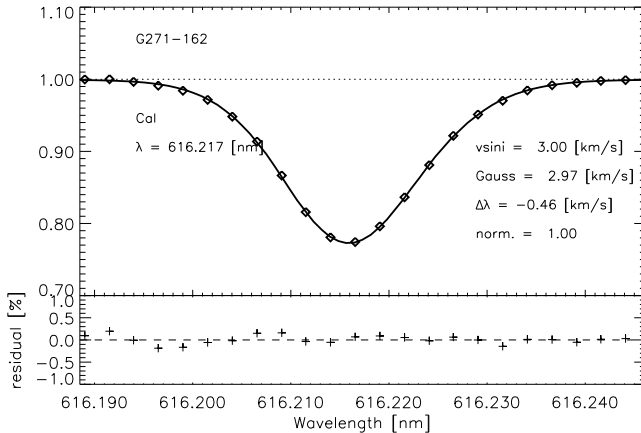


**Fig. 3.** The predicted (solid line) and observed (diamonds) Ca I 616.2 nm line together with the residual fluxes based on the 3D analysis. The rotational broadening has been included through a disk-integration after which a Gaussian instrumental profile has been applied. Note the excellent ability of the 3D profile to describe the observed red asymmetry of the line not possible with 1D models

ing the FWHM of the Gaussian broadening (1D) and  $v_{\text{rot}} \sin i$  (3D), the abundance and the wavelength zeropoint of the observed spectrum were allowed to vary to optimize the fit (Figs. 2 and 3). The most probable value corresponds to the minimum of  $\chi^2$  and  $\Delta\chi^2 = \chi^2 - \chi^2_{\text{min}} = 1, 4$  and  $9$  represent the  $1$ -,  $2$ - and  $3\sigma$  confidence limits of the determinations. These broadening parameters were subsequently used in a similar  $\chi^2$  analysis of the Li I 670.8 nm line. The free parameters in the comparison between the predicted and observed profile were, besides the  ${}^6\text{Li}$  fraction, the total Li abundance and the wavelength zeropoint of the observed profile. It is emphasized that for each

value of  ${}^6\text{Li}/{}^7\text{Li}$  the other free parameters are optimized to get the smallest possible value of  $\chi^2$ .

The 1D analysis of the K I, Ca I and Fe I lines implies a  $FWHM = 5.9 \pm 0.1 \text{ km s}^{-1}$  of the stellar line broadening function. However, the detailed agreement with the observations are far from perfect (Fig. 2). In particular, the distinct red asymmetry of all lines similar to the solar case (e.g. Asplund et al. 2000) is not accounted for. The result of the  $\chi^2$  analysis of the Li I 670.8 nm doublet suggests a possible detection of  ${}^6\text{Li}$ :  ${}^6\text{Li}/{}^7\text{Li} = 0.02 \pm 0.01$  ( $1\sigma$ ). The minimum  $\chi^2_{\text{red}} = \chi^2/\nu$ , where  $\nu$  is the number of degrees of freedom in the fit, is satisfactory close to 1.

The temperature inhomogeneities and velocity fields in the 3D hydrodynamical model atmospheres introduce characteristic line asymmetries, which for the Sun perfectly describe the observed asymmetries even on an absolute wavelength scale (Asplund et al. 2000). The existence of the predicted line asymmetries in the 3D analysis vastly improves the agreement with the observed profiles for G 271-162 (Fig. 3); other lines show similarly encouraging correspondence. This provides additional support for the realism of the 3D model when describing the real stellar photosphere, as well as giving a higher degree of confidence in the estimate of the lithium isotope ratio. The stellar rotation was determined to be  $v_{\text{rot}} \sin i = 2.9 \pm 0.1 \text{ km s}^{-1}$ , which in turn implies  ${}^6\text{Li}/{}^7\text{Li} = 0.02 \pm 0.01$  ( $1\sigma$ ) according to Fig 5, the same result as in the 1D analysis. Again, the minimum  $\chi^2_{\text{red}}$  is close to 1 as it should.

#### 4. Discussion and conclusions

Both the 1D and 3D analyses suggest a possible detection of  ${}^6\text{Li}$  in G 271-162 at the level of  ${}^6\text{Li}/{}^7\text{Li} = 0.02 \pm 0.01$ . Given the remaining uncertainties in the determination of the stellar

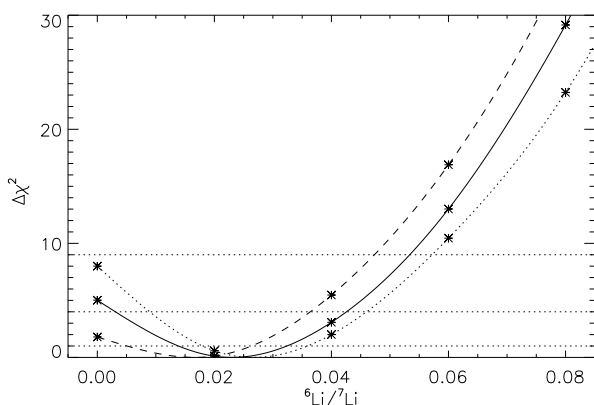


**Fig. 5.** The variation of  $\Delta\chi^2$  in the 3D analysis of the Li 1670.8 nm line as a function of the relative abundance of  ${}^6\text{Li}$  for different adopted  $v_{\text{rot}} \sin i$ : 2.7 (dotted), 2.9 (solid) and 3.1  $\text{km s}^{-1}$  (dashed). The corresponding estimates of  ${}^6\text{Li}/{}^7\text{Li}$  are  $0.027 \pm 0.009$ ,  $0.023 \pm 0.009$  and  $0.017 \pm 0.010$ , respectively. The widths of K I, Ca I and Fe I lines imply  $v_{\text{rot}} \sin i = 2.9 \pm 0.1 \text{ km s}^{-1}$ . The horizontal lines represent the formal  $1\sigma$ ,  $2\sigma$  and  $3\sigma$  confidence limits

line broadening (e.g. NLTE effects) the detection should, however, be considered preliminary. The similarity between the 1D and 3D results and the excellent agreement between the observed and predicted profiles in 3D, could be interpreted as support for a positive detection though. It also lends added confidence to previous detections of  ${}^6\text{Li}$  in metal-poor stars based on 1D investigations (e.g. Smith et al. 1998; Nissen et al. 1999). Evidently, the convective line asymmetries are rather negligible compared to the isotopic shift of the  ${}^6\text{Li}$  doublet.

Regardless of whether  ${}^6\text{Li}$  has been detected in G 271-162 or not, the  ${}^6\text{Li}/{}^7\text{Li}$  ratio appears in any case to be smaller than in HD 84937 for which a weighted average of the results of Hobbs & Thorburn (1997), Smith et al. (1998) and Cayrel et al. (1999) is  ${}^6\text{Li}/{}^7\text{Li} = 0.059 \pm 0.016$  ( $1\sigma$ ). This is quite puzzling, because the two stars have almost identical parameters according to the *uvby*- $\beta$  photometry of Schuster & Nissen (1988). Table 1 lists the measured indices for the three halo stars with  ${}^6\text{Li}$  measurements after correction for a small reddening of G 271-162,  $E(b - y) = 0.020$ , as derived from the  $\beta - (b - y)_0$  calibration of Schuster & Nissen (1989). Table 2 shows the derived parameters using the IRFM calibration of  $T_{\text{eff}}$  vs.  $(b - y)_0$  by Alonso et al. (1996a), the [Fe/H] calibration of Schuster & Nissen (1989) and the  $M_V$  calibration of Nissen & Schuster (1991). The directly measured IRFM temperatures of HD 84937 and BD +26 3578 are 6330 and 6310 (Alonso et al. 1996b) in excellent agreement with the values in Table 2, whereas G 271-162 has not been measured. The absolute magnitude of HD 84937 from the Hipparcos parallax (ESA, 1997) is  $M_V = 3.82 \pm 0.19$  in good agreement with the photometric value within the quoted errors. For the two other stars the relative error of the Hipparcos parallax is far too large to estimate  $M_V$  with any reasonable accuracy. Finally, a preliminary

**Table 1.** Strömgren photometry from Schuster & Nissen (1988)

ID	$V$	$(b - y)_0$	$m_0$	$c_0$	$\beta$
HD 84937	8.33	0.303	0.056	0.354	2.613
G 271-162	10.35	0.306	0.055	0.355	2.602
BD +26 3578	9.37	0.308	0.045	0.366	2.600

**Table 2.** Stellar parameters and Li isotope ratios

ID	$T_{\text{eff}}$	[Fe/H]	$M_V$	${}^6\text{Li}/{}^7\text{Li}$
HD 84937	6315 K	-2.14	3.58	$0.059 \pm 0.016$
G 271-162	6295 K	-2.15	3.53	$0.020 \pm 0.010$
BD +26 3578	6280 K	-2.60	3.08	$0.050 \pm 0.030$

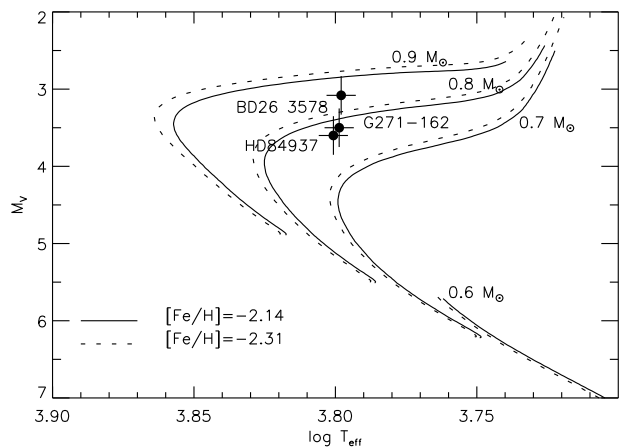


**Fig. 6.** The position of HD 84937, BD+26 3578 and G 271-162 in the  $M_V$ - $\log T_{\text{eff}}$  diagram compared to evolutionary tracks from VandenBerg et al. (2000) with masses and metallicities indicated

abundance analysis shows that HD 84937 and G 271-162 have the same metal abundances within  $\pm 0.15$  dex.

Fig. 6 shows the location of the three stars in the  $M_V$ - $\log T_{\text{eff}}$  diagram. Clearly, HD 84937 and G 271-162 have nearly the same mass. This makes it difficult to explain the lower  ${}^6\text{Li}$  abundance in G 271-162 as a depletion effect and raises the interesting question of a possible intrinsic scatter of  ${}^6\text{Li}/{}^7\text{Li}$  in the ISM at a given metallicity. In this connection we note that some models for the formation of the light elements by cosmic ray processes in the early Galaxy predict a scatter of one order of magnitude in the abundance of  ${}^6\text{Li}$ , Be and B relative to Fe, e.g. the bimodal superbubble model of Parizot & Drury (1999) and the supernovae-driven chemical evolution model for the Galactic halo by Suzuki et al. (1999).

It is clear that the ability of UVES on VLT/Kueyen to gather high quality, high resolution and very high  $S/N$  spectra of even  $V \simeq 10^m 5$  stars as evident from the present study, has opened up the possibility for a large survey of  ${}^6\text{Li}/{}^7\text{Li}$  for stars with a wide range of metallicities. An observing program with this exact aim using UVES/VLT is currently in progress, which is

expected to be of great importance both for an improved understanding of Big Bang nucleosynthesis, cosmic chemical evolution of the light elements and stellar mixing events.

*Acknowledgements.* We are greatly indebted to all the people involved in the conception, construction and commissioning of the UVES instrument, without whom this project would have been impossible.

## References

Alonso A., Arribas S., Martínez-Roger C., 1996a, A&A 313, 873  
 Alonso A., Arribas S., Martínez-Roger C., 1996b, A&AS 117, 227  
 Asplund M., Gustafsson B., Kiselman D., Eriksson K., 1997, A&A  
     318, 521  
 Asplund M., Nordlund Å., Trampedach R., Stein R.F., 1999, A&A  
     346, L17  
 Asplund M., Carlsson M., 2000, submitted to A&A  
 Asplund M., Nordlund Å., Trampedach R., Allende Prieto C., Stein  
     R.F., 2000, submitted to A&A  
 Cayrel R., Spite M., Spite F., et al., 1999, A&A 343, 923  
 D'Odorico S., Kaper L., 2000, UVES User Manual, ESO Doc. no  
     VLT-MAN-ESO-13200-1825  
 ESA, 1997, *The Hipparcos and Tycho Catalogues*, ESA SP-1200  
 Hobbs L.M., Thorburn J.A., 1997, ApJ 491, 772  
 Nissen P.E., Lambert D.L., Primas F., Smith V.V., 1999, A&A 348,  
     211  
 Nissen P.E., Schuster W.J., 1991, A&A 251, 457  
 Parizot E., Drury L., 1999, A&A 349, 673  
 Ryan S.G., Norris J.E., Beers T.C., 1999, ApJ 523, 654  
 Schuster W.J., Nissen P.E., 1988, A&AS 73, 225  
 Schuster W.J., Nissen P.E., 1989, A&A 221, 65  
 Smith V.V., Lambert D.L., Nissen P.E., 1993, ApJ 408, 262  
 Smith V.V., Lambert D.L., Nissen P.E., 1998, ApJ 506, 405  
 Stein R.F., Nordlund Å., 1998, ApJ 499, 914  
 Suzuki T.K., Yoshii Y., Kajino T., 1999, ApJ 522, L125  
 VandenBerg D.A., Swenson F.J., Rogers F.J., Iglesias C.A., Alexander  
     D.R., 2000, ApJ 532, 430